| CHEOPS | Demonstration of improved processes for charge transport layer and PK film deposition leading to an increased $V_{OC}$ of 5% and an increased FF by 2% absolute with a PK layer homogeneity leading to LBIC map variation smaller than 5% on a 5x5 $cm^2$ surface | Deliverable Number **D1.2** |
|---|---|---|
| Project Number **653296** | | Version **1** |

H2020-LCE-2015-1

**CHEOPS – Production technology to achieve low Cost and Highly Efficient phOtovoltaic Perovskite Solar cells**

# Deliverable D1.2

# Demonstration of improved processes for charge transport layer and PK film deposition leading to an increased $V_{OC}$ of 5% and an increased FF by 2% absolute with a PK layer homogeneity leading to LBIC map variation smaller than 5% on a 5x5 $cm^2$ surface

WP1 – Perovskite single junction development

**Authors:** Fabio Matteocci (CHOSE), Luigi Vesce (CHOSE)
Luigi Castriotta (CHOSE), Aldo Di Carlo (CHOSE)

**Lead participant:** CHOSE

**Delivery date:** 13.07.2017

**Dissemination level:** Public

**Type:** Demonstrator

This project has received funding from the European Union's Horizon 2020 research and innovation programme under grant agreement No. 653296.

# Revision History

| **Author Name, Partner short name** | **Description** | **Date** |
|---|---|---|
| Fabio Matteocci (CHOSE) Aldo Di Carlo (CHOSE) and co-authors | Draft deliverable | 30/06/2017 |
| Arnaud Walter (CSEM)<br>Soo-Jin Moon (CSEM) | Revision 1 | 10/07/2017 |
| Fabio Matteocci (CHOSE)<br>Aldo Di Carlo (CHOSE) | Final version | 13/07/2017 |

# Contents

## Acronyms

| | |
|---|---|
| **BL** | Blocking layer |
| **CHOSE** | Università di Roma Tor Vergata |
| **CSEM** | Centre Suisse d'Electronique et de Microtechnique |
| **EPFL** | École Polytechnique Fédérale de Lausanne |
| **ETL** | Electron transport layer |
| **FF** | Fill factor |
| **Fraunhofer** | Fraunhofer Institute for Applied Polymer Research |
| **H2020** | Horizon 2020 |
| **HTL** | Hole transport layer |
| **INERIS** | Institut National de l'Environnement et des Risques |
| **LBIC** | Light beam induced current |
| **MERCK** | Merck KGaA |
| **OXPV** | Oxford Photovoltaics Ltd. |
| **PCE** | Power conversion efficiency |
| **PK** | Perovskite |
| **PV** | Photovoltaic |
| **SC** | Spray cycle |
| **SD** | Standard deviation |
| **SEM** | Scanning electron microscopy |
| **SMART** | SmartGreenScans |
| **SPD** | Spray pyrolysis deposition |
| **TYNDALL-UCC** | Tyndall Nationall Institute |
| **UOXF** | University of Oxford |
| **USAL** | University of Salford |
| **$V_{oc}$** | Open circuit voltage |
| **WP** | Work package |

# Executive Summary

This Deliverable focusses on the development and characterisation of perovskite (PK) solar modules with a total substrate area of 5x5$cm^2$. In particular, we report on the optimisation of the charge transport layers and the PK layer in order to increase the photovoltaic performance and the homogeneity of the deposition. We can highlight the main goals of the deliverable as follows:

1. Realisation of PK modules with improved PV performance
2. Characterisation and testing of the layer homogeneity

## Need for the Deliverable

The improvement of photovoltaic parameters and the homogeneous deposition of PK on an area much larger (5x5 $cm^2$) than the typical test cells is an important requirement for the further development of the project and to achieve the final scaling-up objective of CHEOPS. To reach the goals of the deliverable, we performed a study of the parameters that affect $V_{OC}$ and FF of the PK modules. Furthermore, the requirement on the PK deposition homogeneity led us to a better control of the growth mechanism of the PK layer on the (large) substrate area and to the choice of a proper deposition technique. In particular, the blade coating technique, which is less dependent on the substrate size, here replaces the spin-coating deposition, generally used to realise small area cells.

## Objectives of the Deliverable

We realised high efficient PK modules with improved PV performance:

- Improved processes for charge transport layer and PK film deposition leading to an increased $V_{OC}$ of 5% and an increased FF by 2% absolute
- PK layer homogeneity leading to LBIC map variation smaller than 5% on a 5x5 $cm^2$ surface

## Outcomes

The optimisation of the BL-$TiO_2$ thickness (20-30 nm) leads to $V_{OC}$ increase up to +14% and to a FF increase up to +3% with respect to the standard thickness (40-50nm) used before the CHEOPS project. Furthermore, high uniform LBIC maps have been obtained by using optimised deposition methods. In particular, by using a two-step deposition of the perovskite and using the blade coating to deposit the $PbI_2$ layer and the Spiro-OMeTAD, we accomplished the deliverable goals maintaining the relative standard deviation of LBIC data on the entire active area of the module within 5%.

## Next steps

- Enhancement of the photovoltaic performance by improving the perovskite formulation passing from methylammonium based perovskite to mixed cation perovskites with optimised morphologies and thickness.
- Scale up the process on larger substrate up to 10x10 $cm^2$ for fully bladed modules using automated deposition equipment.
- Design of new layouts for PK modules at high aspect ratio by using optimised P1-P2-P3 laser patterning.

# 1 Increased charge transport layers/perovskite properties

## 1.1 Optimisation of the ETL properties

The Electron Transporting Layer (ETL) is a crucial layer for the realisation of high efficient PK devices. The optimisation of the optical/electrical properties of the ETL layer is mandatory to facilitate the injection of the photo-generated electrons from the perovskite layer to the photo-anode electrode blocking the recombination of the holes between FTO and perovskite layer. In our case, we used a compact $TiO_2$ blocking layer (BL-$TiO_2$) as ETL realised by spray pyrolysis deposition (SPD). The BL-$TiO_2$ properties in terms of surface coverage and thickness play a key role on the working mechanism of the layer. In particular, we consider the realisation of a thinner BL-$TiO_2$ with respect to the conventional one to enhance the light harvesting of the PK layer due to the increased transmittance of the BL-$TiO_2$. However, reducing the thickness of this ETL may lead to a non-uniform coverage of the photoelectrode (glass/FTO) and to the formation of pin-holes. This in turn will increase charge recombination at the photo-electrode affecting the $V_{OC}$ and FF of the device. Thus, the reduction of BL-$TiO_2$ thickness should be accompanied to an improved deposition to guarantee a complete and uniform coverage of the FTO.

In our experiment, the thickness of the BL-$TiO_2$ is optimised by varying the number (N) of spray cycles (SC) during the SPD, while all the other parameters (carrier gas, pressure, solution, deposition speed) are fixed. Our standard process, as reported in our recent paper [1], has a 40-50nm-thick BL-$TiO_2$ layers obtained with N=15 SCs. To achieve the deliverable objectives, we consider to reduce N to 10 which leads to a BL-$TiO_2$ thickness equal to 20-30nm. The BL-$TiO_2$ thicknesses are measured by profilometer as shown in Figure 1a and b for 10 and 15 SCs, respectively.

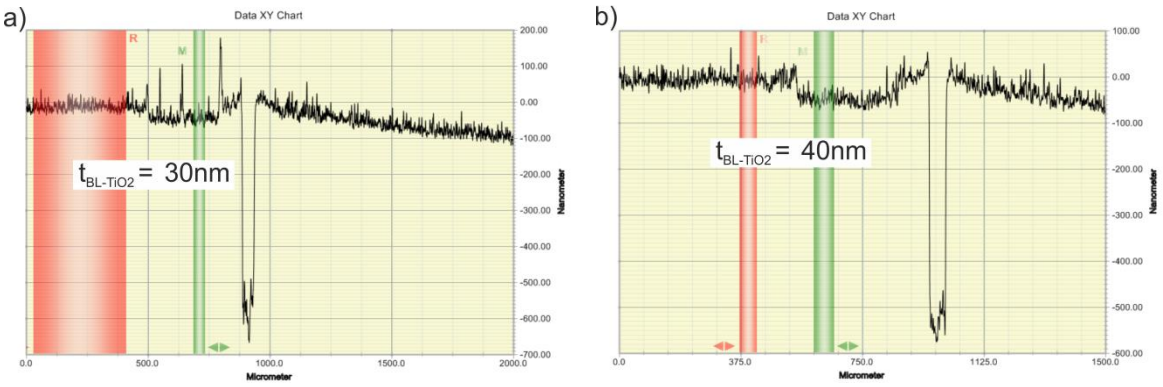


**Figure 1.** Profilometer scans of the BL-$TiO_2$ layers obtained varying the number of spray cycles: a) 20-30nm, N=10 and b) 40-50 nm, N=15.

A batch of four PK modules is realised for each BL-$TiO_2$ thickness. The modules are fabricated with the same device architecture to evaluate the impact of the BL-$TiO_2$ thickness only. The device stack is FTO/BL-$TiO_2$/mp-$TiO_2$/$CH_3NH_3PbI_3$/Spiro-OMeTAD/Au. The results show a remarkable effect of the thickness on the PV performance of the devices especially affecting the $V_{OC}$ and FF values as resumed in Table 1. At 20-30nm, the $V_{OC}$ and FF of the modules are remarkably increased with respect to standard thickness (40-50nm). This could be ascribed to the perfect matching between optical and electrical properties as explained before. Furthermore, the results showed a slight increase of the $I_{SC}$

due to the increased transparency of the substrate at low BL-$TiO_2$ thickness as shown in Figure 2 where the transmittance spectra related to the BL-$TiO_2$ thicknesses are reported.

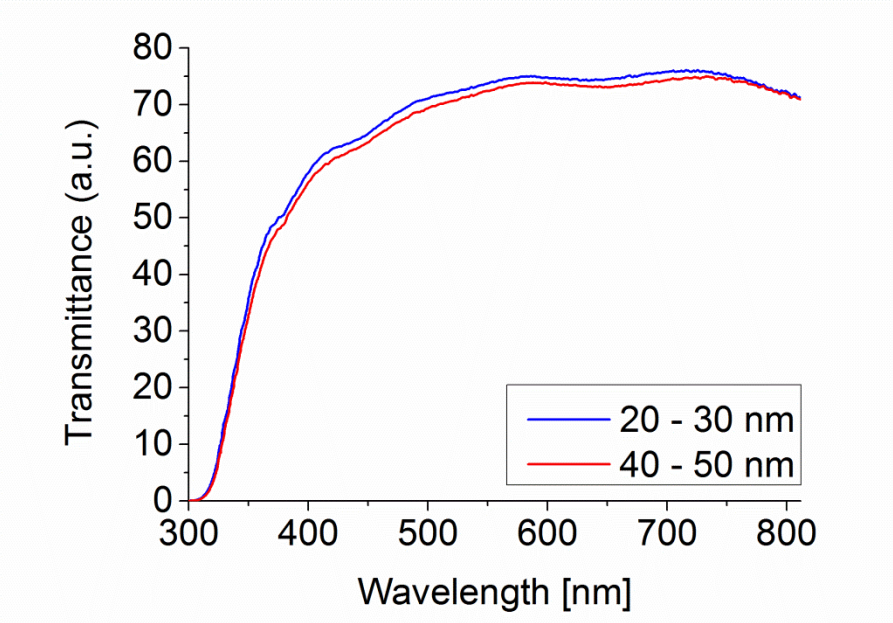


**Figure 2.** Transmittance spectra of the BL-$TiO_2$ layers: 20-30 nm (Blue curve), 40-50 nm (Red Curve)

The relative increase of the PV performance is also confirmed by comparing the average values calculated from the batches of four modules.

The relative $V_{OC}$ increase due to the thickness reduction of the BL- $TiO_2$ is equal to +10.36% and +14.6% comparing the best values and average values, respectively. In both cases the experiment leads to the results expected from the deliverable goals exceeding the +5% as relative $V_{OC}$ increase. Furthermore, the second goal related to the absolute increase of the FF by 2% is also confirmed for best and average values reaching 7.91% and 3.79%, respectively. In Figure 2, the I-V characterisations of the best modules for each thickness are also reported. It is important to remark that the PV performance of this module can be increased by optimising the deposition of the perovskite layer by using blade coating technique.

**Table 1.** Photovoltaic Parameters of the PK modules varying the BL-$TiO_2$ thickness

| | **BL-$TiO_2$ Thickness** | **$V_{oc}$ (V)** | **$I_{sc}$ (mA)** | **FF (%)** | **PCE on active area (%)** | **$V_{oc}$ Relative Variation** | **FF Absolute Variation** |
|---|---|---|---|---|---|---|---|
| **Best values** | 20-30nm | 5.296 | -50.167 | 68.595 | 12.82 | +10.36% (>5%) | +7.91% (>2%) |
| | 40-50nm | 4.799 | -47.566 | 60.687 | 10.03 | | |
| **Average values** (Four PK modules) | 20-30nm | 5.202 ± 0.075 | -50.19 ± 2.34 | 64.38 ± 3.99 | 12.20 ± 1.15 | +14.6% (>5%) | +3.79% (>2%) |
| | 40-50nm | 4.538 ± 0.180 | -47.38 ± 1.29 | 60.59 ± 1.96 | 9.33 ± 0.48 | | |

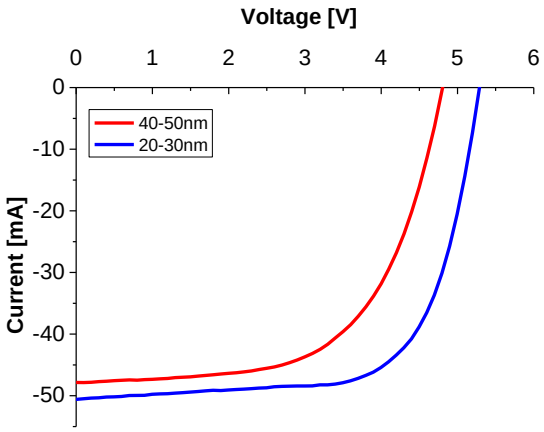


**Figure 3.** I-V characteristics of the PK modules varying the BL-$TiO_2$ thickness: 20-30nm (blue curve), 40-50nm (red curve)

## 1.2 PK and Spiro-OMeTAD depositions by Blade Coating

The $CH_3NH_3PbI_3$-based modules are realised by using the two-step procedure. In order to scale up the realisation procedure of the PK layer, an automated blade coating machine is used to uniformly deposit the $PbI_2$ layer on 5x5$cm^2$ substrate. The $PbI_2$ solution adopted for this process contains 350mg/ml of $PbI_2$ and 15mg/ml of MAI in DMF solvent.

The blade coating technique substantially involves spreading through a moving sharp blade onto a stationary substrate. After this step the solvent in the film is quickly dried by employing an air flow over the substrate. In particular, the preliminary process is based on the following steps:

1) Positioning of a loading glass
2) Pipetting 70 µl of solution on the glass
3) Blade the $PbI_2$ solution over the sample
4) Air-flow drying
5) Dip the sample in the MAI solution for 10min
6) Rinse the sample with IPA
7) Heat the sample at 100 °C for 5mins

The material flows and spreads starting from the loading glass, crossing the sample and finishing on the waste glass. During the levelling time the material can uniformly distribute over the glass, avoiding thickness differences and big pin-holes. The air-flow permits to limit inhomogeneous perovskites morphologies during the subsequent conversion step. In Figure 4a-b, the pictures of both $PbI_2$ and $CH_3NH_3PbI_3$ layers are reported.

a) 


b) 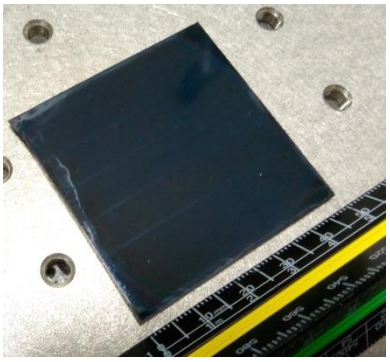

**Figure 4.** Pictures of the perovskite layer deposited by blade coating prior and after the perovskite conversion: a) $PbI_2$ layer and b) $CH_3NH_3PbI_3$ Perovskite.

Moreover, the cross sectional SEM image of the device stack is reported in Figure 5 in order to evaluate the morphologies and the thicknesses of the constituent layers of the device realised by using blade coating technique for both PK and Spiro-OMeTAD layers.

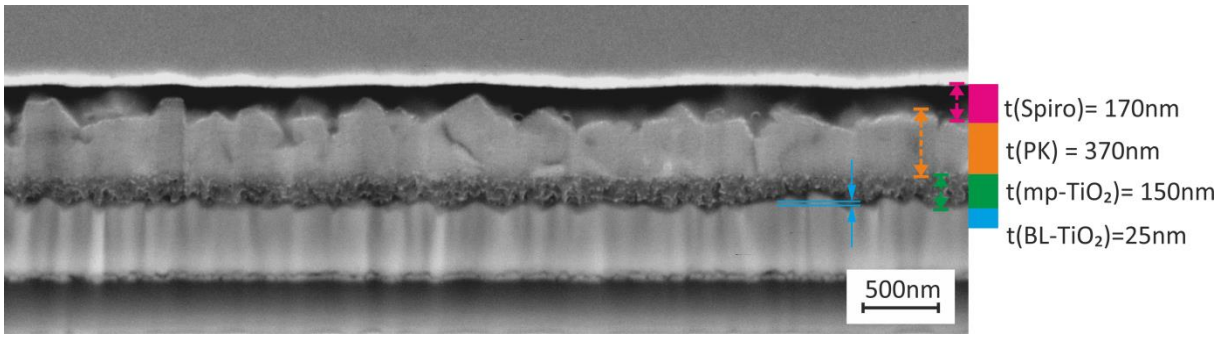


**Figure 5.** Cross sectional SEM image of the optimised device stack.

The cross sectional SEM shows a uniform coverage of the perovskite on the entire range of the measurement with overlayer thickness of 370nm (520nm also considering the mp-$TiO_2$ thickness of 150nm). The Spiro layer was deposited by blade coating technique showing a layer thickness of 170nm. The BL-$TiO_2$ thickness was also measured to be 25nm by SEM analysis confirming the result obtained by profilometer.

## 2 Spatial Uniformity of the PK modules

The spatial uniformity of PK device is one of the main issues to overcome during the scaling up of the device. The perovskite/HTL depositions are very sensitive to the realisation technique, the curing and the annealing steps. In order to evaluate the constraints related to the uniformity, spatial characterisation of the PK homogeneity is mandatory to analyse the defects induced by the realisation process. Several spatially resolved PV characterisation methods are available such as electroluminescence, photoluminescence, lock-in thermography and light beam induced current (LBIC) measurements. LBIC is a non-disruptive technique able to perform a fine characterisation of

the morphology and the uniformity of the active layers forming the device stack by measuring the photocurrent induced by the light beam.

In our LBIC measurement [2] the light beam is moved on the sample to scan the entire aperture area. Spatially resolved photocurrent maps were measured by means of an inverted microscope (Leica DMI 5000) coupled with a monochromator (Cornestone 130) illuminated by a 200 Watt Xenon Lamp. The wavelength was fixed to 530nm (+/-2nm). A long working distance objective with 100x of magnification yielded a 50x50µm spot area. The device area was scanned in steps of 500µm by an x-y motorised stage. A calibrated silicon photodiode was mounted with a beam splitter at the optical entrance of the microscope in order to monitor the incident optical power. The short circuit photocurrents of both the devices and the calibrated photodiode were discriminated by a phase sensitive detection system composed by an optical chopper (177Hz of modulation) and two digital lock-in amplifiers (Eg&g 7265).

## 2.1 LBIC results

We designed the experiment in order to evaluate the uniformity of the perovskite solar modules based on $CH_3NH_3PbI_3$ perovskite and Spiro-OMeTAD as HTL layer. We realised the modules starting for the results obtained from the optimisation of the ETL using blade-coated perovskite. As reference, we also realised single-step based module by using spin-coating technique and solvent quenching method [3] in order to compare the LBIC maps obtained using both deposition procedures. The photocurrent maps obtained for each cell forming the module are normalised with respect the mean value. A distribution histogram of the normalised current for the entire active area of the device is plotted for each map in order to evaluate the homogeneity of the deposition on the entire module. The distribution histograms of the LBIC data are fitted as a Gaussian distribution. The standard deviation (SD) is then used to evaluate the map variation as requested in the deliverable.

The LBIC maps are coloured in graded red scale and plotted in the entire variation range of the averaged photocurrent in order to better evaluate the presence of colour gradient. The light red regions correspond to the local spots of the modules at lower photocurrent. Instead, the deep red regions indicate the areas at higher photocurrent. The presence of these regions indicates a map variation with respect to the mean value of the photo-induced current. The vertical light red region between two adjacent cells of the module is related to the interconnection area (non–active area).

The non-homogeneous spots, in the active area, can be directly referred to the properties of the deposition technique or to the presence of local defects in the constituent layers where the module presents a photocurrent remarkably lower than the average value.

**Table 2.** LBIC map of the PK modules realised depositing both PK and Spiro-OMeTAD layer by spin coating. A Solvent Quenching method is used for the PK deposition.

***Module SS (Spin-coated Perovskite, Spin-Coated Spiro-OMeTAD)***

Aperture Area: 14.93 $cm^2$

Active Area: 13.59 $cm^2$

ETL: BL-$TiO_2$ by SPD (20-30nm)

Perovskite: Spin Coating (S), $CH_3NH_3PbI_3$, Solvent Quenching method

Spiro-OMeTAD: Spin Coating (S)

Conversion Efficiency: 10% on active area, 9.1% on aperture area

*LBIC Map*

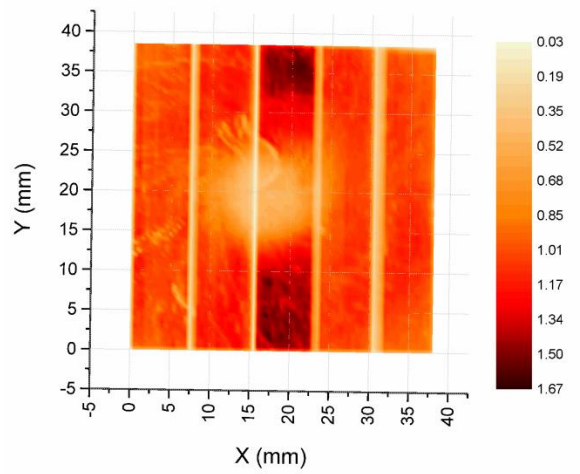


*Normal Distribution Graph*

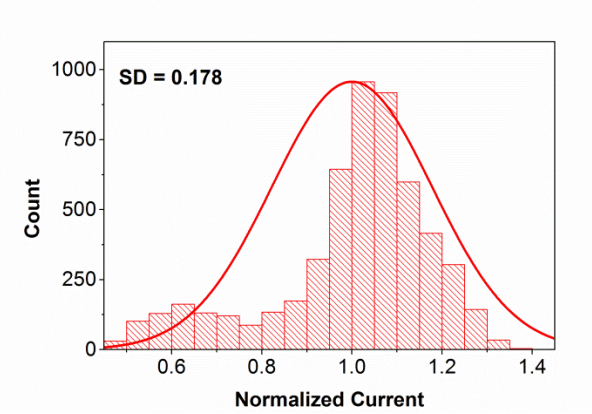

**Table 3.** LBIC Map of the PK modules realised depositing the perovskite layer by blade coating and Spiro-OMeTAD layer by spin coating.

***Module BS (Blade-coated Perovskite, Spin-Coated Spiro-OMeTAD)***

Aperture Area: 15.61 $cm^2$

Active Area: 14.21 $cm^2$

ETL: BL-$TiO_2$ by SPD (20-30nm)

Perovskite Deposition: Blade Coating (B), $CH_3NH_3PbI_3$, Two-step method,

Spiro-OMeTAD Deposition: Spin Coating (S)

Efficiency: 12.8% on active area, 11.7% on aperture area

*LBIC Map*

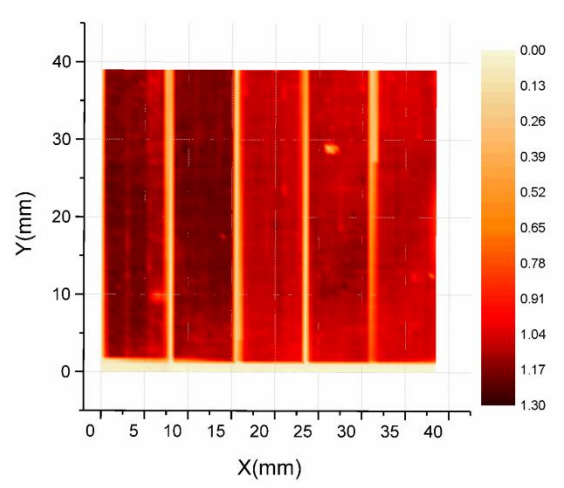


*Normal Distribution Graph*

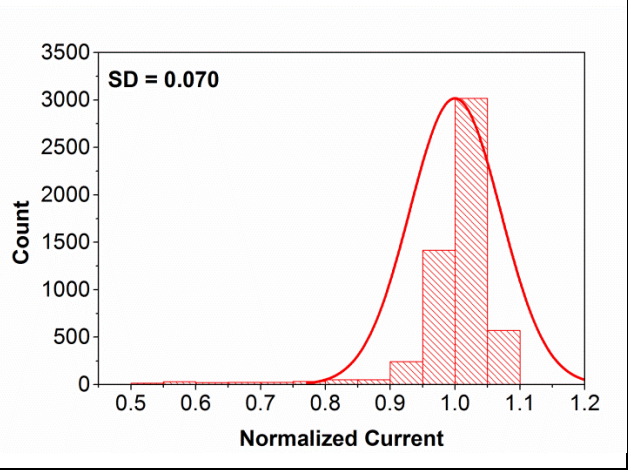

**Table 4.** LBIC map of the PK modules realised depositing both perovskite and Spiro layer by blade coating.

***Module BB (Blade-coated Perovskite, Blade-Coated Spiro-OMeTAD)***

Aperture Area: 15.14 $cm^2$

Active Area: 13.78 $cm^2$

ETL: BL-$TiO_2$ by SPD (20-30nm)

Perovskite Deposition: Blade Coating (B), $CH_3NH_3PbI_3$, Two-step method,

Spiro-OMeTAD Deposition: Blade Coating (B)

Efficiency: 12.6% on active area, 11.5% on aperture area

*LBIC Map*

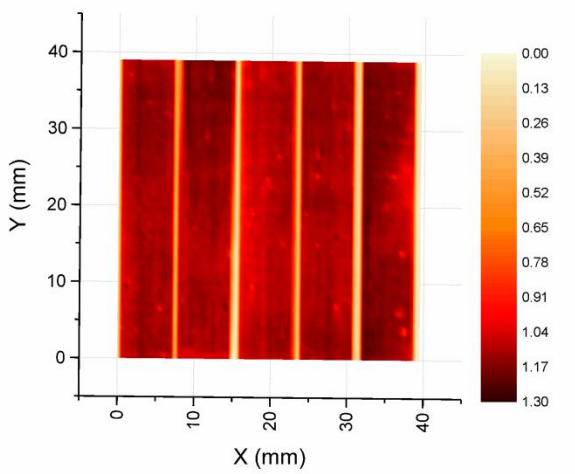


*Normal Distribution Graph*

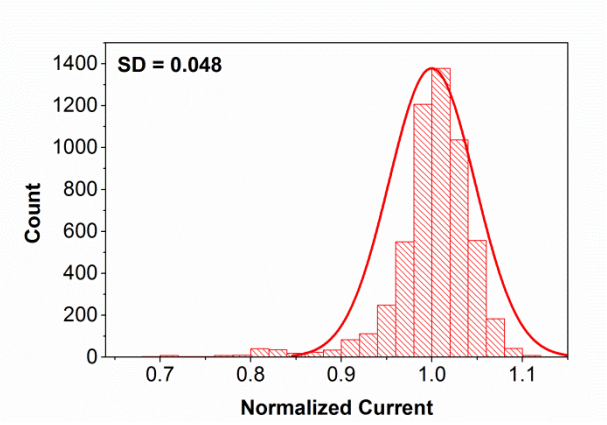

## 2.2 Discussion

The LBIC characterisation pointed out important features regarding the uniformity of the perovskite solar modules realised using two main deposition procedures: single-step deposition and two-step deposition. The single-step deposition is based on the solvent quenching method where an anti-solvent is dripped on the perovskite surface in order to easily wash out the DMF/DMSO solvents prior the perovskite growth. The deposition is realised in air using diethyl ether as an anti-solvent and spin coating technique.

The LBIC results showed large non-uniform region in the middle of the surface related to the effect of the anti-solvent quenching (module SS). In fact, the solvent quenching method is highly dependent on the dripping timing and the amount of the anti-solvent during the spin coating program. Although the module shows PCE equal to 10%, the homogeneity goal is not accomplished resulting in a higher standard deviation (equal to 10%) associated to the normal dispersion of the LBIC data. This is evidence that the solvent quenching method cannot easily scaled for the realisation of perovskite solar modules with high uniformity and reproducibility. On the contrary, the modules fabricated by using the two-step procedure and the automated blade coater are quite uniform in terms of LBIC maps in the whole scanned area demonstrating the effectiveness of the deposition procedure and the curing steps. Moreover, the blade-coating technique leads to high uniform PK layers made in air without controlling the environment during the realisation and it permits a facile up-scaling to larger substrate. Some localised defects are visible on the active area mainly due to the non-uniform coverage of the Spiro-OMeTAD deposition realised by spin coating technique (module BS). Furthermore, the HTM deposition was also improved by using blade coating technique also for the Spiro-OMeTAD deposition (module BB). The PV results show similar photovoltaic performance in terms of PCE (12.8% vs. 12.6%) between the BS and BB modules, however, BB module has an improved uniformity (see Table 5) with a relative standard deviation (coefficient of variation) of the normal distribution of 4.8%.

**Table 5.** Parameters of the Gaussian curves related to the LBIC maps.

| **Sample** | ***Counts*** | ***Relative Standard Deviation*** |
|---|---|---|
| **Module SS** | 5416 | 17.8 % |
| **Module BS** | 5503 | 7.0 % |
| **Module BB** | 5600 | 4.8 % |

# 3 References

[1] F. Matteocci *et al.* Nano Energy 30 (2016) 162–172

[2] L. Cinà *et al.* Energies (2016), 9, 686

[3] N.J. Jeon, *et al.* Nat. Mater. 13 (2014) 897–903.